Bioactive Materials 6 (2021) 823–835

Contents lists available at ScienceDirect

Bioactive Materials

journal homepage: http://www.keaipublishing.com/biomat

Bioglass enhances the production of exosomes and improves their capability of promoting vascularization

Zhi Wu[a,b], Dan He[a,b], Haiyan Li[a,b,*]

[a] Shanghai Jiao Tong University Affiliated Sixth People's Hospital, School of Biomedical Engineering, Shanghai Jiao Tong University, 1954 Huashan Road, Shanghai, 200030, China

[b] Med-X Research Institute, School of Biomedical Engineering, Shanghai Jiao Tong University, 1954 Huashan Road, Shanghai, 200030, China

ARTICLE INFO

Keywords:
Exosomes
Bioglass ion products
Vascularization
Regenerative medicine

ABSTRACT

Recently, exosomes have been extensively applied in tissue regeneration. However, their practical applications are severely restricted by the limited exosome secretion capability of cells. Therefore, developing strategies to enhance the production of exosomes and improve their biological function attracts great interest. Studies have shown that biomaterials can significantly enhance the paracrine effects of cells and exosomes are the main signal carriers of intercellular paracrine communication, thus biomaterials are considered to affect the exosome secretion of cells and their biological function. In this study, a widely recognized biomaterial, 45S5 Bioglass® (BG), is used to create a mild and cell-friendly microenvironment for mesenchymal stem cells (MSCs) with its ion products. Results showed that BG ion products can significantly improve exosome production of MSCs by up-regulating the expression of neutral sphingomyelinase-2 (nSMase2) and Rab27a which enhanced the nSMases and Rab GTPases pathways, respectively. Besides, microRNA analysis indicates that BG ion products can modulate the cargoes of MSCs-derived exosomes by decreasing microRNA-342-5p level while increasing microRNA-1290 level. Subsequently, the function of exosomes is modified as their capabilities of promoting the vascularization of endothelial cells and facilitating the intradermal angiogenesis are enhanced. Taken together, BG ion products are confirmed to enhance exosome production and simultaneously improve exosome function, suggesting a feasible approach to improve the practical application of exosomes in regenerative medicine.

1. Introduction

Exosomes are 30–150 nm sized extracellular vesicles released from living cells after fusion of multivesicular bodies (MVBs) with the plasma membrane and play vital roles in intercellular paracrine communications and numerous biological processes [1–3]. Exosomes have been extensively studied and applied for tissue repair and regeneration owing to their advantages of high stability in circulation, low immune rejection, good targeting effects and multifunctional capacities of regulating recipient cell behaviors [4–8]. For instance, Su et al. found that exosomes released by bone marrow mesenchymal stem cells (MSCs) could be taken up by adipocytes, myocytes and hepatocytes, eventually resulting in insulin resistance *in vitro* and *in vivo* [9]. MSC-derived exosomes have been demonstrated to be able to promote the proliferation and infiltration of chondrocytes and modulate immune reactivity [10]. By attenuating the apoptosis of chondrocytes and enhancing the matrix synthesis of collagen II and VI at the defect region, MSC-derived exosomes can significantly repair and regenerate critical size osteochondral defects [10]. Wang and their team reported that exosomes secreted by human-induced pluripotent stem cells-derived MSCs could be used for many vascularized tissue repair by promoting angiogenesis, such as limb ischemia, cutaneous wound healing, critical-sized bone defects and osteonecrosis of the femoral head [11–14].

In spite of these achievements, the practical application of exosomes in tissue repair is still severely restricted by the large dose requirements in actual administration [15,16]. On one hand, current methods for exosome extraction and purification are inefficient [17,18]. On the other hand, exosome production capability of cells is associated with many factors, such as the cell types, cell viability, and culture microenvironment. Both of these two reasons result in a big challegen in obtaining enough amounts of exosomes for regenerative medicine

Peer review under responsibility of KeAi Communications Co., Ltd.

* Corresponding author. Shanghai Jiao Tong University Affiliated Sixth People's Hospital, School of Biomedical Engineering, Shanghai Jiao Tong University, 1954 Huashan Road, Shanghai, 200030, China.

E-mail address: haiyan.li@sjtu.edu.cn (H. Li).

https://doi.org/10.1016/j.bioactmat.2020.09.011
Received 21 July 2020; Received in revised form 16 September 2020; Accepted 16 September 2020

applications. Hence, apart from the improvement and optimization of exosome isolation methods, enhancing exosome production capability of cells by directly modifying cells or adjusting cell microenvironment is another strategy for obtaining enough exosome for regenerative medicine.

Various biological technologies have been used to directly modify cells in order to regulate exosome production capability of cells [19–23]. Literatures have reported that several key proteins and signaling pathways could strikingly affect the progress of exosome biogenesis and release, including the family of neutral sphingomyelinases (nSMases) and the Rab family of small GTPases [24–26]. For example, studies have demonstrated that nSMases could induce the production of ceramide by mediating the hydrolysis of sphingomyelin. Therefore, the formation of vesicles by coalescing small micro-domains into larger domains and promoting domain-induced budding could be induced [25,26]. Hsu et al. found that Rab35 could obviously regulate exosome secretion which acted as the downstream effector of a series of Tre/Bub 2/Cdc 16 proteins [20]. Ostrowski et al. reported that Rab27a and Rab27b had a key role in exosome secretion by promoting the targeting of multivesicular endosomes to the cell periphery and their docking at the plasma membrane [27]. Although these strategies showed certain efficiency in adjusting exosome production capability of cells, they were heavily dependent on the regulation of protein and signaling pathways through overexpression and knockdown of representative genes, which not only lack of flexible operability in practical applications but also are very expensive.

Numerous reports have demonstrated that biomaterials can affect both the behaviors of single type of cells and cell-cell interactions [28–31]. For example, it was reported that porous β-$CaSiO_3$/Poly-D,L-Lactide-Glycolide composite scaffolds could obviously accelerate the rabbit femur defect repair [32]. In addition, our previous works have also demonstrated that bioactive materials, such as electrospun fiber and silicate bioceramics, could prominently regulate a variety of behaviors of single type of cells [33–35]. Therefore, in this study, we proposed that, in addition to the expensive and time consumable biological technologies, engineering technology can also be used to affect cells with microenvironment created by bioactive materials for adjusting cell exosome production [32,36,37]. Typically, 45S5 Bioglass® (BG), which is composed of 45% SiO_2, 24.5% Na_2O, 24.5% CaO, and 6% P_2O_5 (weight percentage) and recognized as one of the third-generation bioactive inorganic materials, has been widely studied and applied for wound repair [38–41]. Literatures and our previously studies have well demonstrated that BG ion products could obviously promote proliferation and differentiation of various kinds of cells and modulate macrophages polarization [42,43]. Furthermore, our previous studies also confirmed that bioactive silicate ceramics, including BG, could pronouncedly enhance the cell-cell paracrine effects and eventually accelerated wound healing [42–44]. Based on these reports and the facts that exosome production is strongly affected by cell behaviors and exosomes play an important role in intercellular communications with the cargoes they carry, we reason that stimulating cells with bioactive material may be an effective and feasible engineering technology to enhance the production of cell exosome and modify the cells to produce functionalized exosomes for further enhancing tissue regeneration.

Based on those mentioned above, we hypothesized that a strategy could be developed to simultaneously enhance exosome production capability of cells and modify the biological function of the exosomes by biomaterials. Therefore, the purpose of this study was to investigate the effects of biomaterials on cell exosome quantity (production) and quality (cargo). The ion products of 45S5 Bioglass® (BG) were used to stimulate human-derived mesenchymal stem cells (MSCs). The exosome production from MSCs stimulated with or without BG ion products was detected and the function of those exosomes in facilitating the vascularization of human umbilical vein endothelial cells (ECs) was evaluated. Results showed that BG ion products could significantly promote the exosome production from MSCs *via* the enhancement of the nSMases and Rab GTPases pathways. In addition, the cargo analysis of the MSCs-derived exosomes revealed that there were 9 obviously downregulated microRNAs (miRNAs) and 6 upregulated miRNAs in the BG ion products stimulated MSCs-derived exosomes when compared with those in the conventional MSCs-derived exosomes. Furthermore, the MSCs-derived exosomes stimulated by BG ion products showed improved capability of promoting vascularization *in vitro* and angiogenesis *in vivo* as compared to the conventional MSCs-derived exosomes, mainly owing to the significantly downregulated miRNA-342-5p (miR-342-5p) and upregulated miRNA-1290 (miR-1290) in the cargoes of BG ion products stimulated MSCs-derived exosomes. These results well clarify our hypothesis that BG ion products can significantly enhance the production of exosomes and simultaneously improve their biological function. Our findings also suggest that using biomaterials to stimulate cells is a cell-friendly and feasible approach to regulate exosome secretion and improve their practical application in regenerative medicine.

2. Results

2.1. Identification of MSCs-Derived exosomes

Images obtained from transmission electron microscopy (TEM) and high sensitivity flow cytometry (HSFCM) detection clearly revealed that both BG ion products stimulated-MSCs-derived exosomes (BG^+-exo) and conventional cultured MSCs-derived exosomes (Ctrl-exo) exhibited typical round- or cup-like shaped small membrane vesicles (indicated by arrows in Fig. 1a and b) with a size distribution of 50–110 nm and a mean size of 70 ± 5 nm (Fig. 1c and d). Western blot analyses indicated that ubiquitous exosome markers, including CD9, CD63 and Tsg101 proteins, were enriched in both BG^+-exo and Ctrl-exo (Fig. 1e). Besides, the exosome-excluded endoplasmic protein Grp94 was hardly detected in the two exosome groups. In addition, purity assessment results indicated that the percentage of vesicles in the collected MSCs-derived exosomes reached to 93% in two groups, suggesting the high purity of the collected exosomes (Fig. 1f). Taken together, the collected vesicles were identified as typical exosomes and there was no significant difference between BG^+-exo and Ctrl-exo in terms of their morphology, size distribution, marker proteins and vesicle purity.

2.2. BG ion products enhance the production of MSCs-Derived exosomes

Fig. 2a–d showed the effects of BG ion products on the MSCs-derived exosome production. The exosome production was revealed by acetylcholinesterase (AChE) concentration and exosome particle concentrations detected by various kinds of methods. As shown in Fig. 2a, the AChE concentration in the culture supernatant of the two groups increased with time and gradual accumulated. For the first 12 h, there was no obvious difference between the two groups. Interestingly, after 12 h, the accumulative AChE concentration in the BG^+-exo group maintained a continuous upward trend and was significantly higher than that in the Ctrl-exo group in the following 60 h ($p < 0.01$).

Exosome particle concentrations in the culture supernatant were further detected with nanoparticle tracking analysis (NTA). These results displayed a similar trend of concentration changes with the AChE activity changes in supernatant, where no difference was observed in the first 12 h between the two groups but the exosome concentrations in BG^+-exo group were pronouncedly higher than those in the Ctrl-exo group in the following 60 h (Fig. 2b). To further evaluate the difference of the exosome particle concentrations between two groups, exosome particle concentration in the supernatant of MSCs cultured with medium containing BG ion products or not at 48 h was measured by an EXOCET kit and HSFCM. It can further confirm that the exosome concentration of BG^+-exo group was remarkably higher than that of the Ctrl-exo group (Fig. 2c and d).

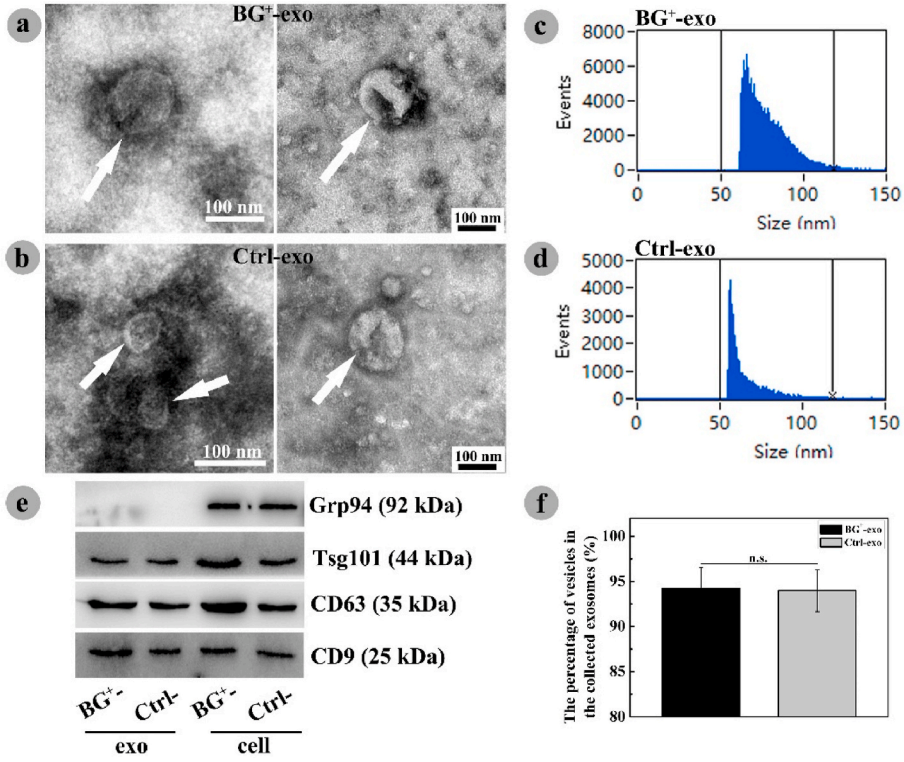

Fig. 1. The effects of BG ion products on the conventional vesicle characteristics of the MSCs-derived exosomes: a,b) regular TEM images (exosomes were indicated by arrows), c,d) size distribution, e) Western blot analysis on the exosome-related marker proteins and f) vesicle purity (%) of the collected BG^+-exo and Ctrl-exo, respectively, and n.s. means no obvious difference.

Exosome internalization was further confirmed by incubating the recipient cell (ECs) with DiO-labeled MSCs-derived exosomes which appeared as green fluorescence dots under 488 nm excitation. It can be seen from Fig. 2e that, after 2 h of incubation, few of the MSCs-derived exosomes, including BG^+-exo and Ctrl-exo, could be taken up and internalized by ECs. After 6 h of incubation, the exosome particles in ECs were obviously accumulated and increased with time and many exosomes were observed in ECs after 12 h of incubation. At all points in time, there were no significant difference between the two groups in terms of the exosome internalization (Fig. S1).

Taken together, it can be concluded that BG ion products could enhance the exosome production of MSCs without significantly changing the internalization of MSCs-derived exosomes by ECs.

2.3. BG ion products enhance exosome production dependent on nSMase2 and Rab27a

Since our study revealed that BG ion products could enhance the exosome production capability of cells, the underlying mechanism was further explored. Firstly, the results displayed that the siRNA transfection treatment, including Lipofectamine® 2000 treatment, negative control siRNA (NC) transfection and scrambled siRNAs transfection, would not significantly affect the gene expression of nSMase2 and Rab27a in MSCs (Fig. S2). In addition, the gene expression of nSMase2 and Rab27a in MSCs transfected with NC exhibited no obvious difference with that in MSCs transfected with the corresponding scrambled siRNA. Therefore, NC was used as the control in this study to replace the scrambled siRNAs control. Then, the results in Fig. 3a–c showed that, after MSCs were stimulated by BG ion products for 48 h, the gene expression and protein secretion of nSMase2 were significantly upregulated when compared with those in the NC group ($p < 0.05$). Similarly, the gene expression and protein synthesis of Rab27a in MSCs treated with BG ion products were also strikingly up-regulated (Fig. 3d–f, $p < 0.05$). After MSCs were treated with nSMase2-small-interfering RNA (siRNA) or Rab27a-siRNA, the gene expressions and protein synthesis of nSMase2 and Rab27a in MSCs were obviously downregulated and showed no obvious difference with their corresponding siRNA-BG treated group (Fig. 3a–f).

In addition, after MSCs were treated with nSMase2-siRNA or Rab27a-siRNA, the numbers of exosome particles in the culture supernatant of siRNA-transfected MSCs cultured with medium containing BG ion products or not were preferentially decreased and there was no significant difference between the siRNA-treated and siRNA-BG-treated groups (Fig. 3g). Interestingly, the exosome concentrations of siRNAs-administrated MSCs were hardly enhanced even the cells were treated once again by BG ion products when compared with those of NC-treated MSCs (Fig. 3g). In addition, these collected exosome particles were identified by Western blot as they showed clear presence of CD9, CD63 and Tsg101 markers (Fig. 3h). Besides, considering the fact that there were a lot of exosome particles in cytoplasm, the intracellular typical exosome-related proteins of CD9, CD63 and Tsg101 were detected and the result showed that both BG ion products and nSMase2-siRNA and Rab27a-siRNA made no significant difference in the secretion of exosome-related marker proteins in the cells while affecting the generation of exosomes (Fig. 3i, Fig. S3).

Furthermore, the intracellular exosome vesicles, also called as intraluminal vesicles (ILVs), were labeled with DiO. As shown in Fig. 4a, when MSCs were cultured with normal medium (NC-Ctrl group), the ILVs in MSCs, presenting as green fluorescent spots, fairly evenly distributed in cytoplasm. When MSCs were cultured with medium containing BG ion products (NC-BG group), the ILVs in MSCs still well dispersed in cytoplasm with obviously increased quantity. When nSMase2-siRNA-treated MSCs were cultured with medium containing BG ion products or not, the quantity of ILVs in MSCs in these two groups was strikingly decreased when compared with those in NC-Ctrl groups. No obvious difference in the distribution and quantity of ILVs was observed in the two nSMase2-siRNA groups. When Rab27a-siRNA-treated MSCs were cultured with medium containing BG ion products or not, the ILVs in MSCs mostly distributed beside the plasma membrane and no obvious difference was observed in the two groups. However, it can be seen that the quantity of ILVs in these cells treated with Rab27a-siRNA was remarkably increased when compared with the NC-Ctrl group (Fig. 4a). The quantity of ILVs in each group was further measured through fluorescent intensity and the statistics results were

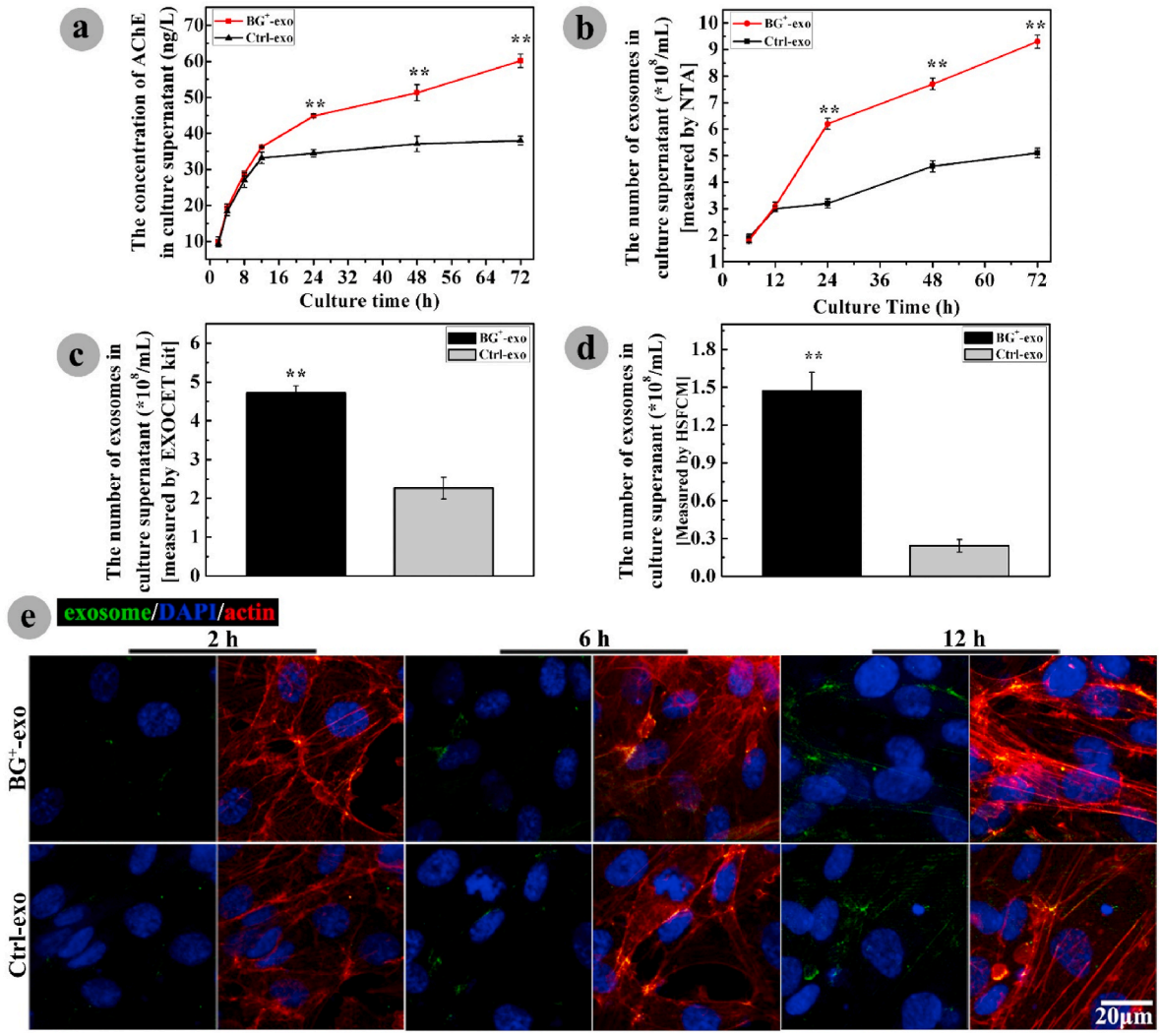

Fig. 2. The effects of BG ion products on the secretion quantity of the MSCs-derived exosomes: a) the AChE concentrations and b) exosome particle concentrations in supernatant after MSCs were cultured with BG ion products for 2–72 h, c,d) the exosome concentrations in supernatant of MSCs stimulated by BG ion products for 48 h, and e) the internalization of MSCs-derived exosomes by ECs (the recipient cells). $^{**}p < 0.01$ means the significant difference when compared with the corresponding control group.

presented in Fig. 4b, suggesting that the quantity of ILVs in NC-BG group and in the two Rab27a-siRNA groups were significantly increased ($p < 0.05$) while those in the two nSMase2-siRNA groups were pronounced decreased ($p < 0.05$) when compared with that in NC-Ctrl group. In addition, the quantity of ILVs in both of the two Rab27a-siRNA groups was preferentially higher than that in NC-BG group ($p < 0.05$). Furthermore, the ILVs in the MSCs culturing with medium containing BG ion products and treated with Rab27a-siRNA (Rab27a-siRNA-BG) showed the highest quantity of ILVs among all groups.

To gain further insight into the mechanisms for enhanced exosome production in MSCs stimulated by BG ion products, an electron microscopic analysis was performed to detect the number of ILVs and MVBs. As shown in Fig. 4c–f, clear MVBs (indicated by arrows in Fig. 4c) and ILVs (the small particles contained in MVBs) could be observed in cytoplasm in each group. The statistics results calculated from images of over 15 single cells were shown in Fig. 4d, revealing that the number of MVBs in a single cell profile in different groups. The number of MVBs in a single cell profile in NC-BG group and the two Rab27a-siRNA groups was much higher than that in a single cell profile in NC-Ctrl group ($p < 0.05$). Besides, among the NC-BG group and the two Rab27a-siRNA groups, the number of MVBs in a single cell profile in Rab27a-siRNA-BG group was highest ($p < 0.05$) while the number of MVBs in a single cell profile in NC-BG group was obviously less than that in a single cell profile in the two Rab27a-siRNA groups ($p < 0.05$).

In addition, the number of ILVs in each MVB was counted and the statistics results were presented in Fig. 4e. It can be seen that the number of ILVs in each MVB of both NC-BG group and Rab27a-siRNA-BG group was significantly higher than that of NC-Ctrl group ($p < 0.05$). However, there was no obvious difference between the NC-BG group and Rab27a-siRNA-BG groups. Moreover, the number of ILVs in each MVB of the two nSMase2-siRNA groups was remarkably decreased when compared with that of NC-Ctrl group ($p < 0.05$). Similarly, there was no obvious difference between the two nSMase2-siRNA groups. Furthermore, the statistics results of the number of ILVs in a single cell profile were shown in Fig. 4f. It can be seen that the number of ILVs in a single cell profile in NC-BG group and the two Rab-27a-siRNA groups was significantly increased ($p < 0.05$) while that in the two nSMase2 groups was significantly reduced ($p < 0.05$) when compared with that in NC-Ctrl group.

In short, BG ion products could significantly enhance the nSMases and Rab GTPase pathways to promote the generation of intracellular exosome vesicles and the release of mature exosomes by upregulating the gene expressions and protein synthesis of nSMase2 and Rab27a, which played crucial roles in the inward budding of endosomal

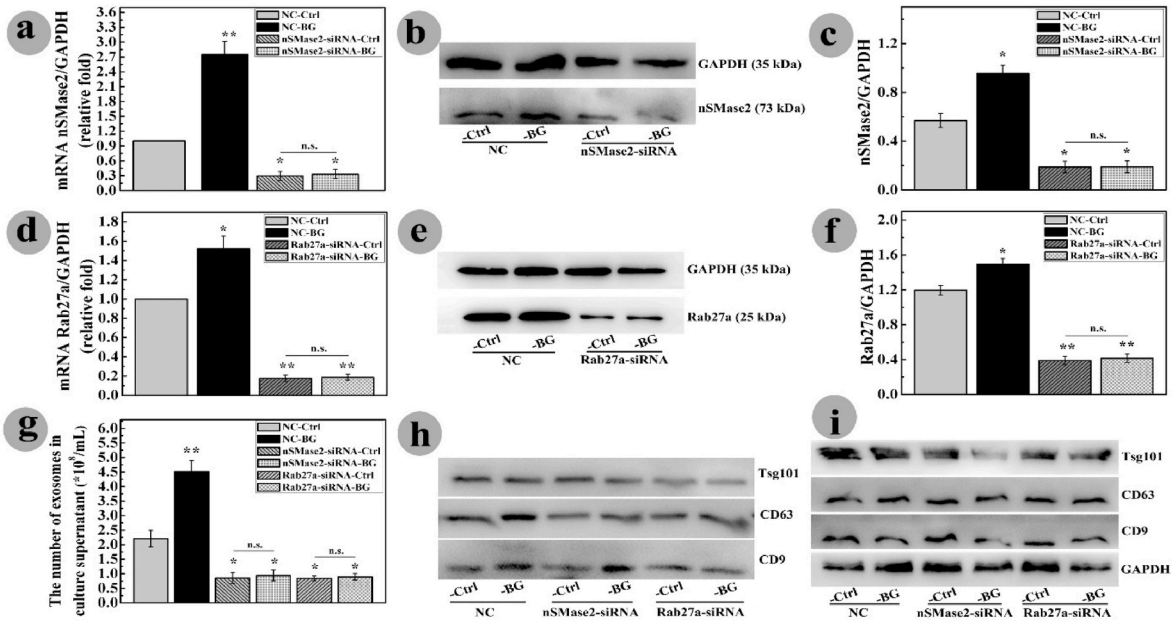

Fig. 3. The role of nSMase2 and Rab27a proteins in BG ion products affecting the production of MSCs-derived exosomes: a-f) The gene expression and protein synthesis of nSMase2 and Rab27a in MSCs, g) the exosome particle concentrations in supernatant, h) the Western blot analysis on the marker proteins of the collected MSCs-derived exosome vesicles and i) the intracellular exosome-related markers in MSCs after MSCs were treated with nSMase2-siRNA or Rab27a-siRNA for 6 h followed by stimulation with BG ion products for 48 h, respectively. $*p < 0.05$ and $**p < 0.01$ mean the significant differences when compared with the corresponding control group, and n.s. means no obvious difference.

compartments to form ILVs, and the docking at and fusion with plasma membrane of MVBs to release exosome vesicles, respectively.

2.4. BG^+-exo accelerate the vascularization of ECs

Vascularization of ECs cultured with different concentrations of BG^+-exo or Ctrl-exo was shown in Fig. 5a and Fig. S4. It can be seen that both of BG^+-exo and Ctrl-exo could induce ECs to elongate and self-assemble into half-circles and even full-circles and eventually form capillary-like networks (indicated by arrows in Fig. 5a and Fig. S4), and these effects were closely associated with the concentrations of exosomes. In addition, BG^+-exo with the concentration of 5×10^9 vesicles mL^{-1} could significantly enhance ECs to form capillary-like networks and generate NO when compared with the Ctrl-exo (Fig. 5b). In Fig. 5c, it can be seen that, as compared to control medium (Ctrl group), medium containing both BG^+-exo and Ctrl-exo could result in significantly upregulated angiogenic-related gene expressions in ECs, including vascular endothelial growth factor (VEGF), VEGF receptor 2 (KDR) and endothelial nitric oxide synthase (eNOS) ($p < 0.05$). Particularly, ECs treated with medium containing BG^+-exo could express much higher level of these genes than those treated with medium containing Ctrl-exo ($p < 0.05$). Moreover, the Western blot results in Fig. 5d revealed that more VEGF and KDR were synthesized in ECs cultured with medium containing BG^+-exo when compared with those in ECs cultured with medium containing Ctrl-exo and the control medium (Ctrl group).

To further evaluate the capability of BG^+-exo in regulating vascularization of ECs, intradermal injection assays for angiogenesis observation were carried out. As shown in Fig. 5e, after the administration of MSCs-derived exosomes, obvious angiogenesis was observed as micro vessels were formed and grown out by budding from the existed blood vessels in the injection region (indicated by arrows in Fig. 5e). The statistics results were shown in Fig. 5f, which revealed that the number of newly formed micro vessels in the two MSCs-derived exosomes administrated groups were significantly higher than that in Sham group ($p < 0.05$). In addition, the number of micro vessels in BG^+-exo group was remarkably higher than that in Ctrl-exo group ($p < 0.05$). The hematoxylin and eosin (H&E) staining images showed many full-circle structures with obvious presence of red blood cells (indicated by arrows in Fig. 5g), which were viewed as micro vessels here. The statistics results in Fig. 5h indicated that more micro vessels were formed in BG^+-exo group than those in other two groups ($p < 0.05$).

The tissue sections were further double immunofluorescence stained with CD31 and α-smooth actin (α-SMA) to identify the micro vessels and the results were shown in Fig. 5i. The results depicted that most ECs in the area of injection skin were aggregated and distributed as distinct circles, which well matched the circle structures in H&E staining images and confirmed that those circle structures were micro vessels. In addition, few obvious smooth muscle cells were observed in those micro vessels, indicating that those micro vessels were newly formed immature blood vessels. Furthermore, more micro-scaled blood vessels could be observed in the skin injected with BG^+-exo than those skins treated with Ctrl-exo and control solution (Sham). The corresponding statistics results were shown in Fig. 5j, summarizing that the number of newly formed immature micro vessels stimulated by BG^+-exo was significantly higher than that stimulated by Ctrl-exo and the Sham group ($p < 0.05$). These results suggested that, BG^+-exo exhibited excellent capability of promoting the vascularization of ECs *in vitro* in a dose-dependent manner and improving the angiogenesis *in vivo*.

2.5. MiRNA analysis

To further elucidate the mechanism through which BG^+-exo enhanced vascularization of ECs, microarray analysis of exosomes secreted by MSCs treated with or without BG ion products were performed and the results were shown in Fig. 6. It can be seen that there was a significant differential expression of 15 candidate miRNAs between the two groups ($p < 0.05$). Among these, 9 miRNAs were downregulated and 6 miRNAs were upregulated in BG^+-exo group when compared with those in Ctrl-exo group (Fig. 6a). In addition, the gene ontology (GO) analysis on the target mRNAs of all the differentially expressed (DE) miRNAs displayed that these target mRNAs could well regulate cell behaviors through affecting biological processes (DNA transcription, RNA translation and ATP and protein kinase

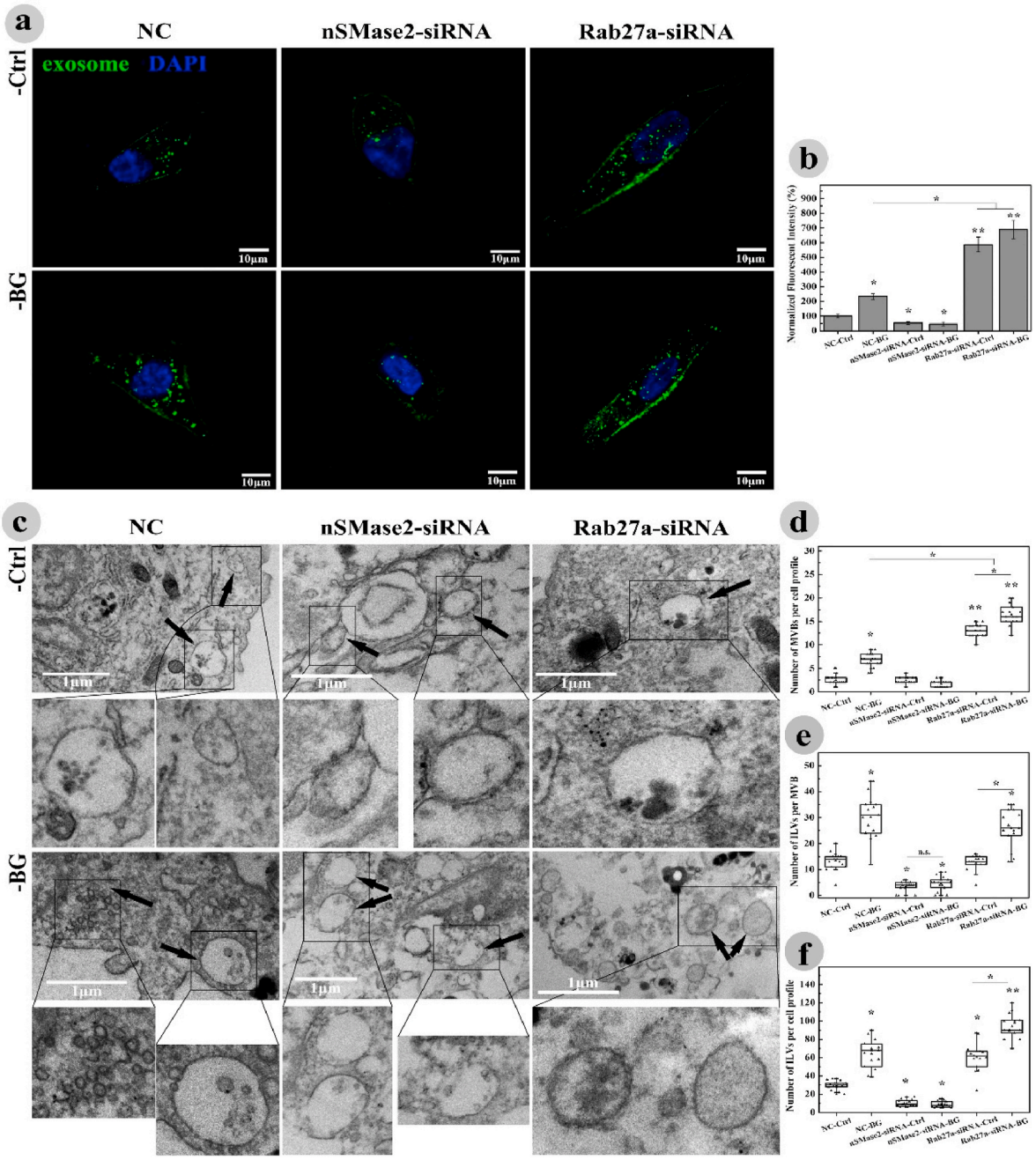

Fig. 4. The rold of nSMase2 and Rab27a proteins in BG ion products affecting the generation and release of MSCs-derived exosomes: a,b) the intracellular exosome vesicles labeled with DiO and their quantitation analysis based on the fluorescent intensity; c-f) representative TEM images of MSCs and the quantitation analysis on the MVBs and ILVs (clear MVBs were shown by arrows and ILVs referred to the small particles contained in MVBs) after MSCs were treated with nSMase2-siRNA or Rab27a-siRNA for 6 h followed by stimulation with BG ion products for 48 h, respectively. $*p < 0.05$ and $**p < 0.01$ mean the significant differences when compared with the corresponding control group or the corresponding two groups and n.s. means no obvious difference.

binding), adjusting cellular component in nucleus, cytosol, cytoplasm and cell junction, and influencing molecular function in DNA transcription, intracellular and intercellular signal transduction, cell differentiation as well as G-protein couple receptor signaling pathway (Fig. 6b).

Moreover, the KEGG signaling pathway enrichment analysis was performed and the results were shown in Fig. 6c, showing that the detected target mRNAs could be enriched in the pathways of regulation of actin cytoskeleton, tight junction, focal adhesion, VEGF signaling pathway and the extensively studied PI3K-Akt and MAPK signaling pathway that could regulate cell behaviors in cell proliferation, cytoskeleton reorganization, cell junction assembly, migration and functional differentiation. Among these signaling pathways, the VEGF signaling pathway, which was widely reported to play an important role in the vascularization of ECs, attracted our attention as it is enrichment score almost reached 3. As miR-342-5p and miR-1290 were related with the VEGF pathway, the relative expression of the miR-342-5p and miR-1290 in the exosomes were detected. It can be seen from in Fig. 6d and e that, when compared with those in Ctrl-exo, the expression level of miR-342-5p and miR-1290 in BG^{+}-exo was 56.4-fold downregulated and 5.6-fold upregulated, respectively.

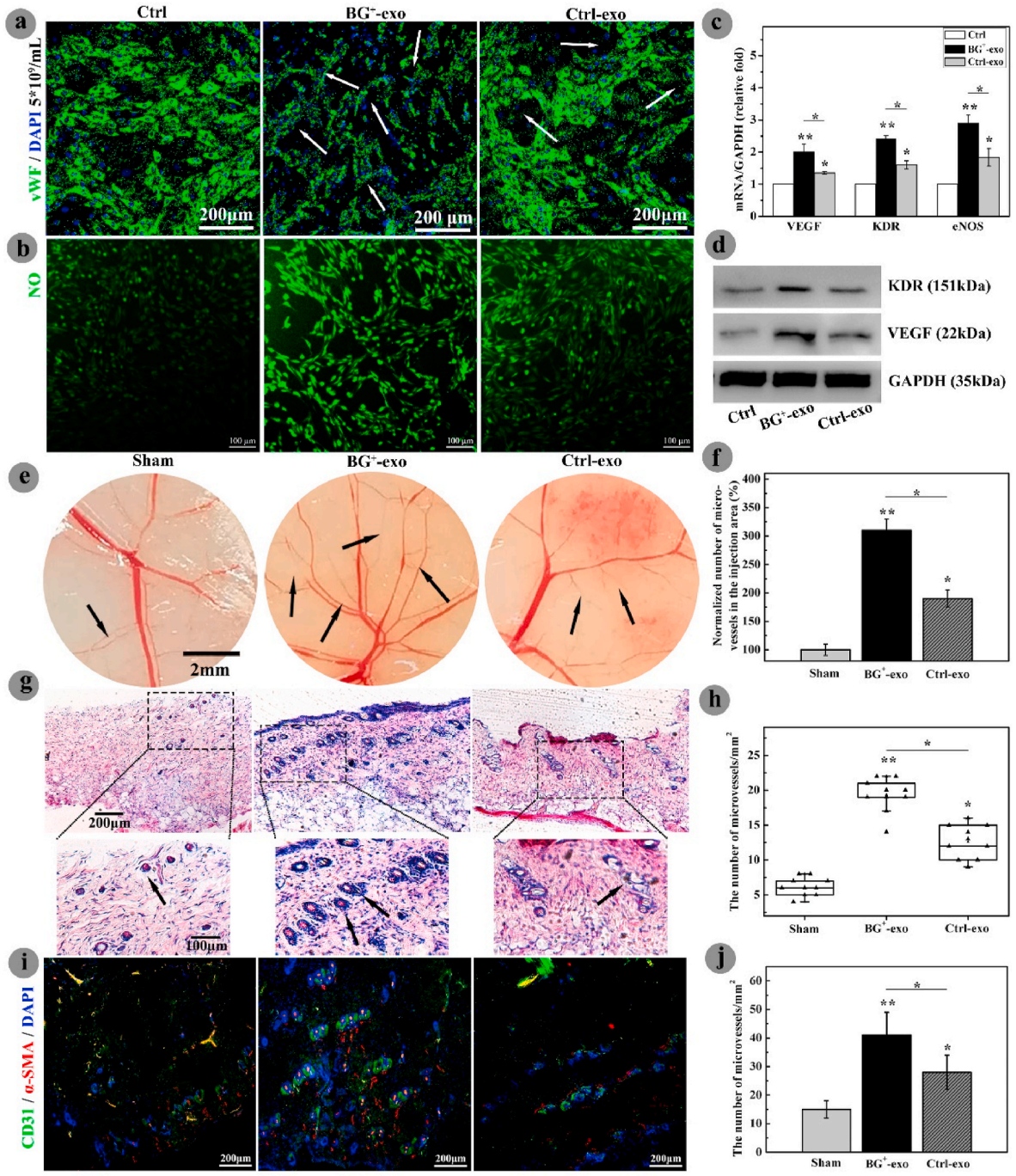

Fig. 5. The effects of BG ion products on the capability of MSCs-derived exosomes in promoting the vascularization of ECs *in vitro* and *in vivo*: a) the vWF staining images, b) NO staining images, c) genes expression of VEGF, KDR and eNOS, and d) protein detection of KDR and VEGF in ECs cultured with MSCs-derived exosomes *in vitro* for 2 d, respectively; e,f) the light-field pictures taken with a camera and the quantitation analysis on the visible microvessels, g,h) the H&E staining images of the skin samples at the injection site and the quantitation analysis on the microvessel-like structures and i,j) the double immunofluorescence images of the skin samples at the injection site stained with CD31 and α-SMA and the quantitation analysis of the labeled microvessels, respectively. $*p < 0.05$ and $**p < 0.01$ mean the significant differences when compared with the corresponding control/sham group.

2.6. BG^+-exo influence the vascularization of ECs via MiR-342-5p and MiR-1290

To validate the function of miR-342-5p and miR-1290 in regulating the vascularization of ECs, miRNA mimics assays were carried out. It showed that after the miRNA transfection, the vascularization effects of ECs were highly correlated with the intracellular level of miR-342-5p and miR-1290. As shown in Fig. 7a and b, the level of miR-342-5p and miR-1290 in ECs was significantly increased when ECs were transfected with the mimics of the corresponding miRNA while that was obviously decreased when ECs were transfected with the inhibitor of the corresponding miRNAs ($p < 0.05$). Notably, when ECs were treated with MSCs-derived exosomes, BG^+-exo significantly increased the miR-1290 level but had no obvious influence on miR-342-5p level in ECs, while Ctrl-exo significantly increased on both miR-342-5p level and miR-1290 level in ECs ($p < 0.05$).

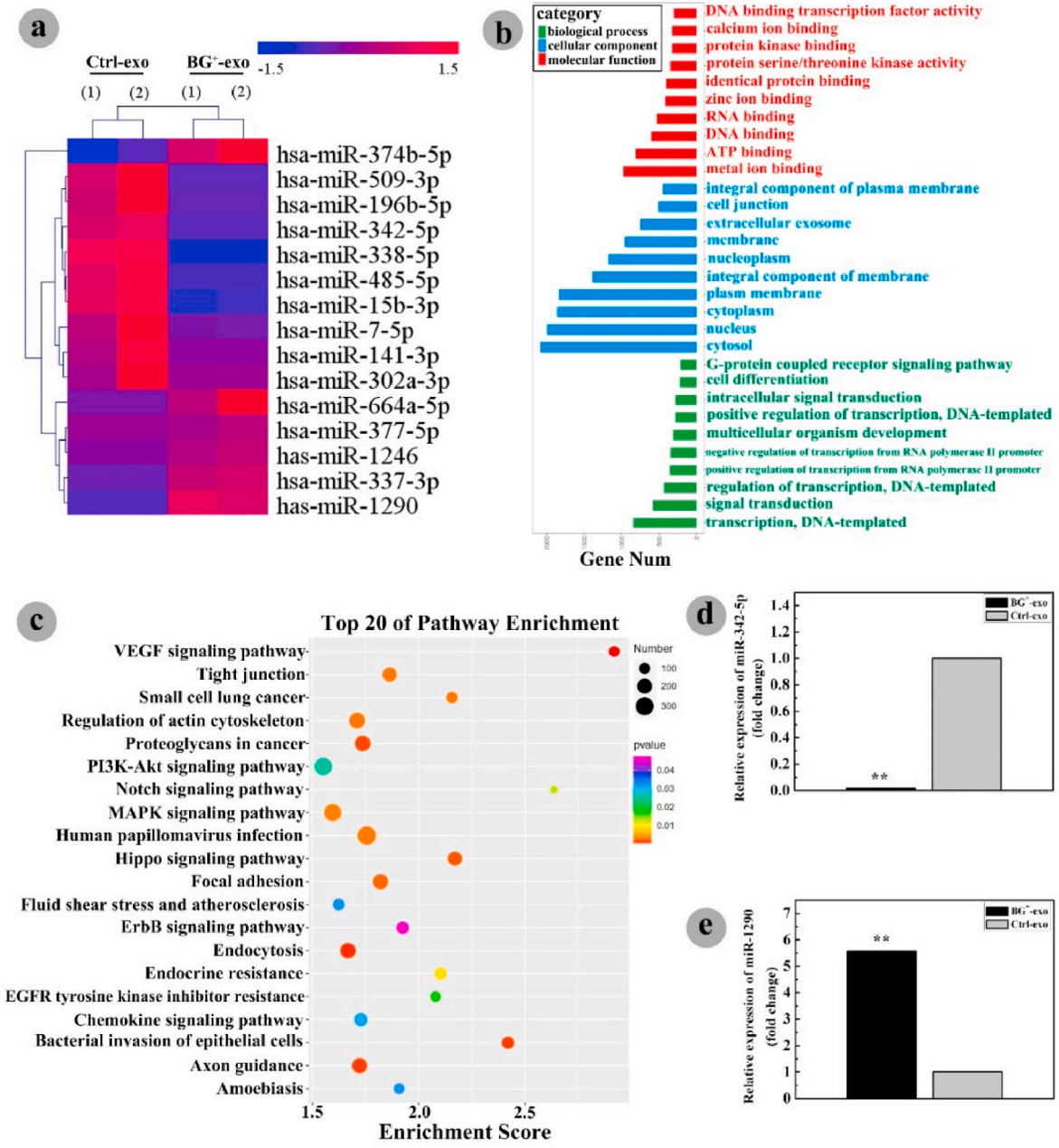

Fig. 6. The effects of BG ion products on the cargoes of MSCs-derived exosomes: a) The heat map of the differently expressed (DE) miRNAs between BG^{+}-exo and Ctrl-exo, b) GO analysis and c) the KEGG signaling pathway enrichment analysis on the target mRNAs of all the DE miRNAs; d-e) the expression of miR-342-5p and miR-1290 in MSCs-derived exosomes responded to the BG ion products stimulation. $^{**}p < 0.01$ means the significant differences when compared with the corresponding control group.

Then, the vWF staining images displayed that the NC mimics and inhibitor had no obvious effects on the growth and distribution of ECs (Fig. 7c). Interestingly, clear semi-circle structures and capillary-like networks were observed when the ECs were transfected with miR-342-5p inhibitor, miR-1290 mimics and their combination. Meanwhile, no obvious circle structures or networks could be observed when ECs were treated with miR-342-5p mimics and miR-1290 inhibitor as well as their combination. In addition, when ECs were treated with miR-342-5p inhibitor, miR-1290 mimics and their combination, obviously more NO was generated and detected in ECs when compared with that in ECs treated with NC mimics (Fig. 7d). These results further confirmed that low level of miR-342-5p and high level of miR-1290 could enhance the vascularization of ECs.

3. Discussion

Recently, due to their advantages of hemodynamic stability, low immunological recognition and sufficient cargoes, exosomes have been extensively studied and applied for diagnosis and treatment of tumors, drugs loading and targeting delivery, as well as tissue repair and regeneration [5,6,45–48]. However, practically, the requirement of high doses of exosomes for tissue repair has been a key challenge and rigorously hindered the application of exosomes because most cells, such as MSCs, exhibited a very limited capability for exosome production under conventional conditions. In addition, the current methods for exosome isolation were inefficient [11,14,49]. Hence, the exploration of a strategy that can enhance the exosome production of cells seems to

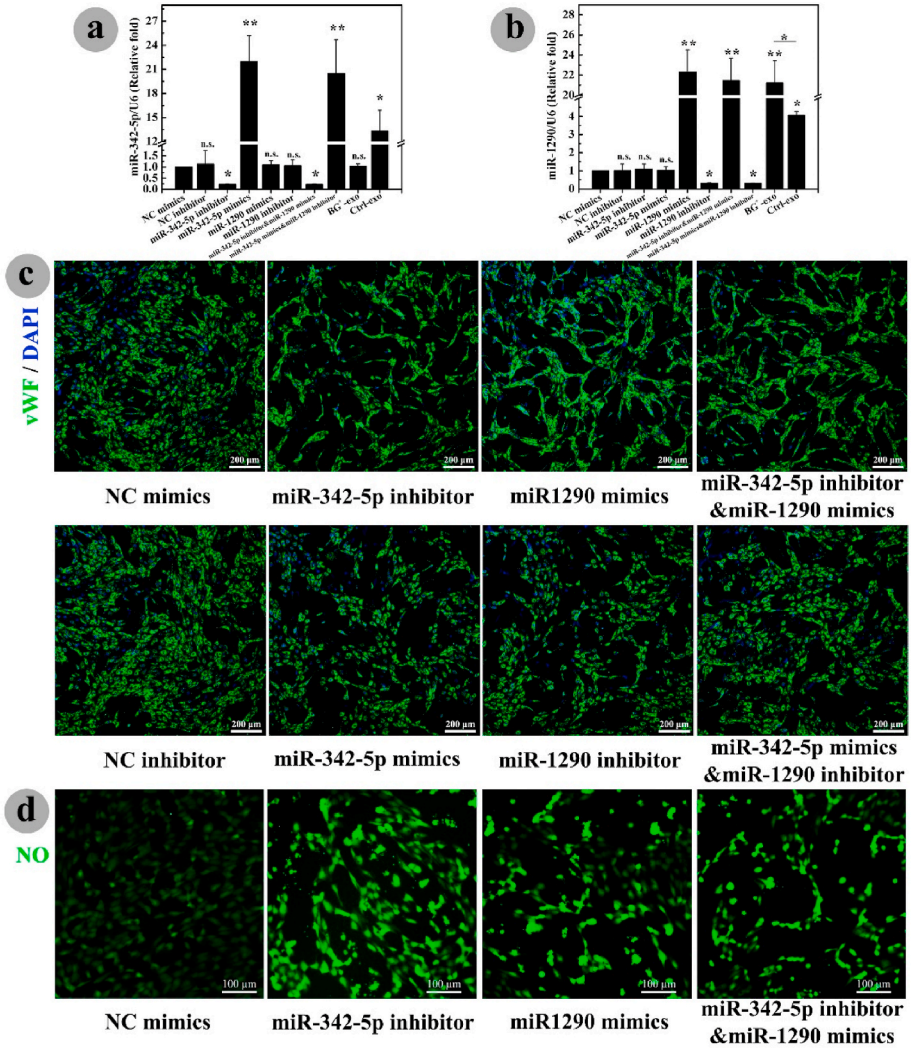

Fig. 7. The functional study of miR-342-5p and miR-1290 in affecting the vascularization of ECs *in vitro*: a,b) the level of miR-342-5p and miR-1290 in ECs, c) vWF staining images and d) NO generation in ECs after ECs were treated with miRNAs mimics or inhibitor or their combination for 2 d, respectively. $*p < 0.05$ and $**p < 0.01$ mean the significant differences when compared with NC mimics group or between the corresponding two groups, and n.s. means no obvious difference when compared with NC mimics group.

be very attractive. Although it has been reported that changes in cell culture conditions, such as hypoxia and low pH microenvironment, can either enhance exosome production/yield or improve the biological activity of the secreted exosomes, it can be difficult to maintain healthy cells under such unfriendly conditions in bioreactors for large scale production [21,50–53]. In the current study, a mild and cell-friendly microenvironment contributed by BG ion products was demonstrated to be able to enhance the exosome production of MSCs without causing any obvious damage to the cells. In addition, the function of MSC-derived exosomes was even improved by BG ion products as the BG^{+}-exo showed higher stimulatory effects on vascularization of ECs than Ctrl-exo. Therefore, in this study, we proposed an effective strategy to promote cells to secrete exosomes and modify the function of exosomes by stimulating the cells with proper biomaterials.

As compared to the previous reported approaches for enhancing exosome production by regulating the progress of exosome biogenesis and release with key proteins and signaling pathways management [20,26,27,54], our strategy is more efficient and feasible in practical applications with low cost since only biomaterials were used to treat the cells. By simply culturing MSCs with medium containing BG ion products, the exosome production capability of MSCs was 2-fold increased without changing the conventional vesicle characteristics of the exosomes, including the morphology, size distribution, marker proteins and internalization (Figs. 1 and 2). It has been widely reported that the family of nSMases and the Rab family of small GTPases pathways play essential roles in the regulation of vesicle formation and membrane traffic. In addition, nSMase2 was one of the members of nSMases family and Rab27a was the most studied protein of Rab GTPases pathway in membrane events, the roles of nSMase2 and Rab27a in the enhancement of exosome production by BG ion products were studied. Furthermore, studies have demonstrated that nSMase2 could promote the formation of ceramide by hydrolytically removing the phosphocholine moiety of sphingomyelin and subsequently accelerated the budding of the endosomal membrane to form intravesicals [24–26,55,56]. As for Rab27a, literatures reported that it was predominantly expressed and located at the CD63-positive multivesicular endosomes and acted as a regulator for the vesicle transport events, including vesicle motility, vesicle docking to specific compartments in cells and a membrane-fusion process [27,57], Therefore, modulating the expression of nSMase2 and Rab27a to control nSMases and Rab GTPases pathways can effectively affect the exosome formation and release, respectively.

In our study, BG ion products could upregulate the expression of nSMase2 and Rab27a in MSCs, which subsequently enhanced the numbers of intracellular MVBs and ILVs as well as the exosome particle

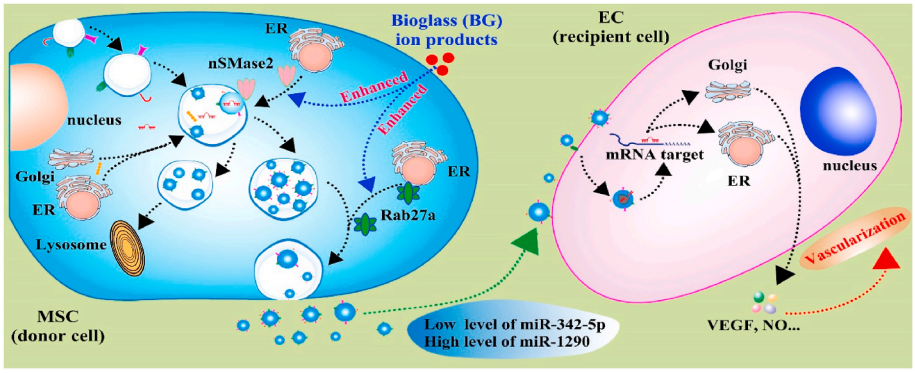

Fig. 8. Proposed underlying mechanisms of BG ion products in enhancing the production and modifying the function of MSCs-derived exosome. We hypothesize that BG ion products enhance MSCs to generate exosomes by upregulating the expression of nSMase2 and promote MSCs to release exosomes by upregulating the expression of Rab27a in MSCs, respectively, and simultaneously enable these exosomes to promote vascularization of ECs with reinforced capability by regulating the levels of miR-342-5p and miR-1290 in cargoes.

concentration in the culture supernatant (Figs. 3 and 4). In addition, the exosome particles released into the culture supernatant were sharply decreased with the downregulated expression of nSMase2 or Rab27a in MSCs by the corresponding siRNA. Simultaneously, the intracellular MVBs and ILVs in MSCs were obviously decreased with the downregulated expression of nSMase2 and pronouncedly increased with the downregulated expression of Rab27a, which was well consistent with those reported in literatures [26,50]. Therefore, after the expression of nSMase2 was downregulated, the intracellular exosome generation and formation were reduced and subsequently the exosome release was decreased. However, after the expression of Rab27a was downregulated, the exosome generation was not affected but the exosome retention and accumulation within cytoplasm were increased, which also resulted in the obvious decrease of exosome release. These results further confirmed that the proteins of nSMase2 and Rab27a played critical roles in exosome production but their roles were different: the nSMase2 and Rab27a protein molecules were responsible for the exosome generation and release, respectively. Notably, after the expression of nSMases and Rab27a were downregulated by siRNAs, the level of exosome vesicles released into extracellular space could hardly be upregulated by BG ion products, which indicated that the two protein molecules were essential for enhancing exosome production by BG ion products.

Interestingly, an additional result was obtained when we detected the biological function of the different exosomes released from MSCs cultured with or without BG ion products. The results demonstrated that the BG ion products could modulate the function of the MSC-derived exosomes as BG^+-exo possessed enhanced capability of facilitating vascularization of ECs and intradermal angiogenesis than the Ctrl-exo (Fig. 5). As is well-known, the biological functions of exosomes were determined by the loaded biological components and information, including growth factors, proteins, DNA, long non-coding RNAs and, in particularly, miRNAs [9,58–61]. MiRNAs, small non-coding RNAs of 18–25 nucleotides, could suppress gene expression to control various biological processes, including cell survival, cell apoptosis, cell cycle and gene regulation in cells [62]. For instance, exosomal miR-132 derived from neurons could regulate brain vascular integrity and acted as a novel avenue for neurovascular communication [63]. In this study, the vascularization capability of ECs was enhanced by the BG^+-exo because the BG^+-exo contained more proangiogenic related miRNAs and less antiangiogenic related miRNAs. Results demonstrated that 9 miRNAs genes were downregulated and 6 miRNAs genes were upregulated in BG^+-exo than in the Ctrl-exo (Fig. 6a). Our results indicated that, among these miRNAs, miR-342-5p played pivotal roles in regulating vascularization of ECs and both low level of miR-342-5p and high level of miR-1290 as well as their combination cold contribute to the enhanced vascularization (Fig. 7). MiR-342-5p was widely studied for its multifunction in mediating the effects and interaction among angiogenic pathways, and miR-1290 was extensively studied for its participation in tumor initiation, invasion and metastasis [64–66]. In addition, it has been reported that miR-342-5p could attenuate VEGF-induced Akt phosphorylation and downregulate the endoglin for inhibiting endothelial cells proliferation and angiogenesis [67–70]. Thus, miR-342-5p can inhibit the vascularization and angiogenesis of ECs. As for miR-1290, it was predominantly reported to act in tumor progression [65,66]. In addition, it has been demonstrated that the upregulated miR-1290 in non-small-cell lung cancer A549 cells could attenuate ischemia/reperfusion induced myocardial apoptosis [71]. Hence miR-1290 may be able to enhance the vascularization of ECs. Therefore, the decreased level of miR-342-5p and increased level of miR-1290 as well as their combination in BG^+-exo may contribute to the enhanced stimulatory effects of BG^+-exo on vascularization.

These results proved that the BG ion products could modulate the cargos of the MSCs-derived exosomes by reducing the level of miR-342-5p and lifting the level of miR-1290, which coordinately stimulated the vascularization of ECs. The proposed underlying mechanisms by which BG ion products enhanced functionalized MSCs-derived exosome production were illustrated in Fig. 8.

4. Conclusion

In this study, we investigated the effects of BG ion products on the exosome production of MSCs and found that BG ion products could significantly promote MSCs to secrete exosomes without changing their morphology, size distribution and internalization. The mechanism studies showed that the proteins of nSMase2 and Rab27a played critical roles in BG ion products enhancing the cell exosome production. In addition, we further demonstrated that the exosome function was modified by BG ion products as the BG^+-exo showed better stimulatory effects on vascularization of ECs than the Ctrl-exo. Furthermore, the exosome cargo analysis showed that BG ion products remarkably downregulated the level of miR-342-5p and upregulated the level of miR-1290 in the BG^+-exo, which contributed the stimulatory effects of BG^+-exo on EC vascularization and intradermal angiogenesis. Taken together, the BG ion products could not only improve exosome production from MSCs but also effectively functionalize the MSC-derived exosomes with enhanced capability of facilitating vascularization.

5. Experimental section

5.1. Cell isolation and culture

Human-derived mesenchymal stem cells (MSCs, Sciencell, USA) were cultured with mesenchymal stem cell medium (MSCM, Sciencell, USA) and human umbilical vein endothelial cells (ECs) were isolated according to previously described methods, and cultured with endothelial culture medium (ECM, Sciencell, USA) [72]. The use of human umbilical cord veins was approved by the donors, and all experiments comply with the current laws of China. See supporting information for details.

5.2. Bioglass ion products preparation

45S5 Bioglass® powders (BG, ~38 μm) were purchased from Kunshan Chinese Technology New Materials Co., Ltd (Kunshan, China). The BG ion products used in this study were prepared according to the method adapted from protocols reported in previous literatures and ISO10993 [42,73]. According to our previous work, BG ion products diluted at 1:128 exhibited the strongest capability to enhance the paracrine effect of cells [42,43,73]. Therefore, in this study, the BG ion products were diluted 128 times with basal MSCM for further use and the concentrations of different types of ions in the BG ion products is shown in Table S2. Details are described in supporting information.

5.3. Exosome isolation and characterization

The isolation and characterization of exosomes in this study follow the latest guidelines from the International Society for Extracellular Vesicles (MISEV2018, PMID 30637094). MSCs were stimulated with BG ion products for 48 h and the released exosomes by MSCs in the supernatant were isolated with a method combining conventional ultracentrifugation and ultrafiltration. The obtained BG stimulated MSCs-derived exosomes were named as BG^{+}-exo and conventionally cultured MSCs-derived exosomes were named as Ctrl-exo, which were stored at −80 °C or used for characterization or further study. The isolated exosomes pellets were further identified by morphological observation, size distribution measurement, Western blot analysis and vesicles purity detection, and the detailed methods are described in supporting information.

5.4. Exosome quantification characterization and internalization

According to the previous reports, acetylcholinesterase (AChE) was enriched in exosomes [54,74]. Hence, firstly, evaluation of AChE activity in cell culture medium with a human AChE Elisa kit (MLBio, China) was carried out to preliminarily investigate the effects of BG ion products on the exosome production. Then, the exosomes released into culture supernatant from MSCs stimulated by BG ion products for 6–72 h were isolated as above and the exosome particle concentration was measured by nanoparticle tracking analysis (NTA, Malvern, UK), an EXOCET exosome quantitation assay kit (System Biosciences, Palo Alto, CA, USA) and the HSFCM device [75–77]. Exosomes released by MSCs cultured with same medium containing no BG ion products were used as the control samples and were detected with the same methods. For the internalization of MSCs-derived exosomes by the recipient cells (ECs), a Transwell assay was undertaken. See supporting information for details.

5.5. Mechanism study on exosome secretion

As reported, the neutral sphingomyelinases (nSMases) pathway and the Rab GTPases pathway played important roles in exosome generation and release [20,26,27]. Herein, we explored if the BG ion products affected MSCs exosome production by affecting these two signaling pathways. Firstly, the expression levels of the key genes in these two signaling pathways, nSMase2 and Rab27a were detected. Then, to further verify the function of nSMase2 and Rab27a in the effects of BG ion products on MSCs exosome production, small-interfering RNA (siRNA) transfection assay was performed, and the gene expression, protein synthesis as well as the exosome generation of MSCs were evaluated. See supporting information for details.

5.6. SiRNA transfection

In order to explore the role of nSMase2 and Rab27a in BG ion products affecting the production of MSCs-derived exosomes, transfection with specific nSMase2 and Rab27a siRNAs in MSCs was performed to downregulate the gene expression of nSMase2 and Rab27a, respectively. After the siRNA transfected-MSCs were treated with BG ion products for 48 h, the gene expression and protein synthesis of nSMase2 and Rab27a in MSCs were detected. In addition, the intracellular exosome generation and exosome release in supernatant were further measured, observed and identified, respectively. The experimental details are described in supporting information.

5.7. Exosomal function study

As mentioned above, the production of exosomes and their biological function are closely associated with the microenvironment of the donor cells. In addition, the co-culture model of cells has also been reported to affect the exosome secretion of cells [78]. Therefore, to avoid the effects of co-culture models on the biological function of exosomes and on the subsequent exosome-cell interactions, MSCs-derived exosomes were directly added to the culture medium of ECs to investigate the effects of BG ion products on the changes of exosome function by studying the interactions of MSC-exosomes and ECs. Then, immunofluorescence staining of von Willebrand factor (vWF), NO staining, gene expression and protein synthesis of vascular endothelial growth factor (VEGF), VEGF receptor 2 (KDR) and endothelial nitric oxide synthase (eNOS) of ECs cultured with MSCs-derived exosomes *in vitro* were carried out. The detailed methods are described in supporting information.

5.8. Analysis of in vivo blood vessel formation

To explore the capability of MSCs-derived exosomes in facilitating the angiogenesis, 50 μL of exosomes-containing PBS solution (5×10^{10} particles mL^{-1}) was subcutaneously injected to the dorsal region of 4-week old male Kun Ming mice to form a stable spheroidal bulge [79]. After 1 week, the skin at injection region of each mouse was obtained to analyze the capillaries on the inner side by photographing, hematoxylin and eosin (H&E) staining and CD31 and α-smooth actin (α-SMA) (Abcam) co-immunofluorescence staining. An Institutional Review Committee of Shanghai Jiao Tong University, School of Biomedical Engineering approved all animal study protocols.

5.9. Exosomal MicroRNA analysis

MSCs-derived exosomes were isolated as described above and the known microRNAs (miRNAs) in the two groups of exosomes were identified and their expression patterns in different samples were analyzed by Shanghai OE Biotech (China). A p value cut-off of 0.05 and a fold-value change of ≥1.5 were used as a filter to identify the differentially expressed (DE) miRNAs. Then gene ontology (GO) analysis and KEGG signaling pathway enrichment analysis of the target mRNA genes of all the DE miRNAs were performed

5.10. MiRNA function study

The function of miRNA-342-5p (miR-342-5p) and miRNA-1290 (miR-1290) in affecting the vascularization of ECs was studied with the miRNA mimics and inhibitors (Shanghai Biogene Co., Ltd, China). The vascularization and NO generation of ECs treated with miRNA mimics or inhibitor was assessed by vWF immunofluorescence staining and DFA-2 staining, respectively. See supporting information for details.

5.11. Statistical analysis

Data were shown as means ± standard deviation (SD). At least three independent experiments were performed and five duplicate samples in each test were set for statistical analysis. A one-way analysis of variance (ANOVA) with Tukey's post hoctest was used for statistical analysis of multiple comparisons. Significant differences with the

control group or the corresponding two groups were considered when $*p < 0.05$ or $**p < 0.01$, and no obvious difference between the corresponding two groups were marked as n.s.

CRediT authorship contribution statement

ZhiWu: Methodology, Formal analysis, Investigation, Writing - original draft, Writing - review &. **Dan He:** Methodology. **Haiyan Li:** Conceptualization, Validation, Resources, Writing - review & editing-.

Declaration of competing interest

The authors declare that they have no known competing financial interests or personal relationships that could have appeared to influence the work reported in this paper.

Acknowledgements

This work was supported by the Natural Science Foundation of China (Grant No. 31771024 and 31971274) and the Interdisciplinary Program of Shanghai Jiao Tong University (Project Number: ZH2018ZDA20).

Appendix A. Supplementary data

Supplementary data to this article can be found online at https://doi.org/10.1016/j.bioactmat.2020.09.011.

References

[1] W. Stoorvogel, M.J. Kleijmeer, H.J. Geuze, G. Raposo, The biogenesis and functions of exosomes, Traffic 3 (2002) 321–330.
[2] M. Mittelbrunn, F. Sánchez-Madrid, Intercellular communication: diverse structures for exchange of genetic information, Nat. Rev. Mol. Cell Biol. 13 (2012) 328–335.
[3] Schneider, M. Simons, Exosomes: vesicular carriers for intercellular communication in neurodegenerative disorders, Cell Tissue Res. 352 (2013) 33–47.
[4] M. Colombo, G. Raposo, C. Théry, Biogenesis, secretion, and intercellular interactions of exosomes and other extracellular vesicles, Annu. Rev. Cell Dev. Biol. 30 (2014) 255–289.
[5] R. Gallet, J. Dawkins, J. Valle, E. Simsolo, G. Couto, R. Middleton, E. Tseliou, D. Luthringer, M. Kreke, R.R. Smith, L. Marbán, B. Ghaleb, E. Marbán, Exosomes secreted by cardiosphere-derived cells reduce scarring, attenuate adverse remodelling, and improve function in acute and chronic porcine myocardial infarction, Eur. Heart J. 38 (2017) 201–211.
[6] X. Ke, D. Yang, J. Liang, X. Wang, S. Wu, X. Wang, C. Hu, Human endothelial progenitor cell-derived exosomes increase proliferation and angiogenesis in cardiac fibroblasts by promoting the mesenchymal-endothelial transition and reducing high mobility group box 1 protein B1 expression, DNA Cell Biol. 36 (2017) 1018–1028.
[7] Park.R. Zhao, A. West, A. Yabuuchi, H. Huo, T.A. Ince, P.H. Lerou, M.W. Lensch, G.Q. Daley, Reprogramming of human somatic cells to pluripotency with defined factors, Nature 451 (2008) 141–148.
[8] S. Bian, L. Zhang, L. Duan, X. Wang, Y. Min, H. Yu, Extracellular vesicles derived from human bone marrow mesenchymal stem cells promote angiogenesis in a rat myocardial infarction model, J. Mol. Med. 92 (2014) 387–397.
[9] T. Su, Y. Xiao, Y. Xiao, Q. Guo, C. Li, Y. Huang, Q. Deng, J. Wen, F. Zhou, X. Luo, Bone marrow mesenchymal stem cells-derived exosomal MiR-29b-3p regulates aging-associated insulin resistance, ACS Nano 13 (2019) 2450–2462.
[10] S. Zhang, S.J. Chuah, R.C. Lai, J.H.P. Hui, S.K. Lim, W.S. Toh, MSC exosomes mediate cartilage repair by enhancing proliferation, attenuating apoptosis and modulating immune reactivity, Biomaterials 156 (2018) 16–27.
[11] G. Hu, Q. Li, X. Niu, B. Hu, J. Liu, S. Zhou, S. Guo, H. Lang, C. Zhang, Y. Wang, Z. Deng, Exosomes secreted by human-induced pluripotent stem cell-derived mesenchymal stem cells attenuate limb ischemia by promoting angiogenesis in mice, Stem Cell Res. Ther. 6 (2015) 10.
[12] J. Zhang, J. Guan, X. Niu, G. Hu, S. Guo, Q. Li, Z. Xie, C. Zhang, Y. Wang, Exosomes released from human induced pluripotent stem cells-derived MSCs facilitate cutaneous wound healing by promoting collagen synthesis and angiogenesis, J. Transl. Med. 13 (2015) 49.
[13] X. Qi, J. Zhang, H. Yuan, Z. Xu, Q. Li, X. Niu, Bin Hu, Yang Wang, X. Li, Exosomes secreted by human-induced pluripotent stem cell-derived mesenchymal stem cells repair critical-sized bone defects through enhanced angiogenesis and osteogenesis in osteoporotic rats, Int. J. Biol. Sci. 12 (2016) 836–849.
[14] X. Liu, Q. Li, X. Niu, B. Hu, S. Chen, W. Song, J. Ding, C. Zhang, Y. Wang, Exosomes secreted from human-induced pluripotent stem cell-derived mesenchymal stem cells prevent osteonecrosis of the femoral head by promoting angiogenesis, Int. J. Biol. Sci. 13 (2017) 232–244.
[15] D.C. Watson, B.C. Yung, C. Bergamaschi, B. Chowdhury, J. Bear, D. Stellas, A. Morales-Kastresana, J.C. Jones, B.K. Felber, X. Chen, G.N. Pavlakis, Scalable, cGMP-compatible purification of extracellular vesicles carrying bioactive human heterodimeric IL-15/lactadherin complexes, J. Extracell. Vesicles 7 (2018) 1442088.
[16] D.B. Patel, C.R. Luthers, M.J. Lerman, J.P. Fisher, S.M. Jay, Enhanced extracellular vesicle production and ethanol-mediated vascularization bioactivity via a 3D-printed scaffold-perfusion bioreactor system, Acta Biomater. 95 (2019) 236–244.
[17] B.J. Tauro, D.W. Greening, R.A. Mathias, H. Ji, S. Mathivanan, A.M. Scott, R.J. Simpson, Comparison of ultracentrifugation, density gradient separation, and immunoaffinity capture methods for isolating human colon cancer cell line LIM1863-derived exosomes, Methods 56 (2012) 293–304.
[18] J.Z. Nordin, Y. Lee, P. Vader, I. Mager, H.J. Johansson, W. Heusermann, O.P. Wiklander, M. Hallbrink, Y. Seow, J.J. Bultema, J. Gilthorpe, T. Davies, P.J. Fairchild, S. Gabrielsson, N.C. Meisner-Kober, J. Lehtio, C.I. Smith, M.J. Wood, S. El Andaloussi, Ultrafiltration with size-exclusion liquid chromatography for high yield isolation of extracellular vesicles preserving intact biophysical and functional properties, Nanomedicine 11 (2015) 879–883.
[19] N. Amzallag, B.J. Passer, D. Allanic, E. Segura, C. Théry, B. Goud, R. Amson, A. Telerman, TSAP6 facilitates the secretion of translationally controlled tumor protein/histamine-releasing factor via a nonclassical pathway, J. Biol. Chem. 279 (2004) 46104–46112.
[20] C. Hsu, Y. Morohashi, S. Yoshimura, N. Manrique-Hoyos, S. Jung, M.A. Lauterbach, M. Bakhti, M. Grønborg, W. Möbius, J. Rhee, F.A. Barr, M. Simons, Regulation of exosome secretion by Rab35 and its GTPase-activating proteins TBC1D10A-C, J. Cell Biol. 189 (2010) 223–232.
[21] H.W. King, M.Z. Michael, J.M. Gleadle, Hypoxic enhancement of exosome release by breast cancer cells, BMC Canc. 12 (2012) 421.
[22] T. Tsunemi, K. Hamada, D. Krainc, ATP13A2/PARK9 regulates secretion of exosomes and alpha-synuclein, J. Neurosci. 34 (2014) 15281–15287.
[23] D.C. Watson, D. Bayik, A. Srivatsan, C. Bergamaschi, A. Valentin, G. Niu, Jenifer Bear, M. Monninger, M. Sun, A. Morales-Kastresana, J.C. Jones, B.K. Felber, X. Chen, I. Gursel, G.N. Pavlakis, Efficient production and enhanced tumor delivery of engineered extracellular vesicles, Biomaterials 105 (2016) 195–205.
[24] F. Schimmöller, I. Simon, S.R. Pfeffer, Rab GTPases, directors of vesicle docking, J. Biol. Chem. 273 (1998) 22161–22164.
[25] C.J. Clarke, C.F. Snook, M. Tani, N. Matmati, N. Marchesini, Y.A. Hannun, The extended family of neutral sphingomyelinases, Biochemistry 45 (2006) 11247–11256.
[26] K. Trajkovic, C. Hsu, S. Chiantia, L. Rajendran, D. Wenzel, F. Wieland, P. Schwille, B. Brügger, M. Simons, Ceramide triggers budding of exosome vesicles into multivesicular endosomes, Science 319 (2008) 1244–1247.
[27] M. Ostrowski, N.B. Carmo, S. Krumeich, I. Fanget, G. Raposo, A. Savina, C.F. Moita, K. Schauer, A.N. Hume, R.P. Freitas, B. Goud, P. Benaroch, N. Hacohen, M. Fukuda, C. Desnos, M.C. Seabra, F. Darchen, S. Amigorena, L.F. Moita, C. Thery, Rab27a and Rab27b control different steps of the exosome secretion pathway, Nat. Cell Biol. 12 (2010) 19–30.
[28] T.H. Qazi, D.J. Mooney, G.N. Duda, S. Geissler, Biomaterials that promote cell-cell interactions enhance the paracrine function of MSCs, Biomaterials 140 (2017) 103–114.
[29] J.S. Fernandes, P. Gentile, R.A. Pires, R.L. Reis, P.V. Hatton, Multifunctional bioactive glass and glass-ceramic biomaterials with antibacterial properties for repair and regeneration of bone tissue, Acta Biomater. 59 (2017) 2–11.
[30] L. Cai, R.E. Dewi, A.B. Goldstone, J.E. Cohen, A.N. Steele, Y.J. Woo, S.C. Heilshorn, Regulating stem cell secretome using injectable hydrogels with in situ network formation, Adv. Healthc. Mater. 5 (2016) 2758–2764.
[31] G. Kaur, F. Baino, J.C. Mauro, V. Kumar, G. Pickrell, N. Sriranganathan, S.G. Waldrop, Biomaterials for Cell Encapsulation: Progress toward Clinical Applications, Clinical Applications of Biomaterials, 2017, pp. 425–458.
[32] C. Wang, K. Lin, J. Chang, J. Sun, Osteogenesis and angiogenesis induced by porous b-$CaSiO_3$/PDLGA composite scaffold via activation of AMPK/ERK1/2 and PI3K/Akt pathways, Biomaterials 34 (2013) 64–77.
[33] H. Yu, J. Peng, Y. Xu, J. Chang, H. Li, Bioglass activated skin tissue engineering constructs for wound healing, ACS Appl. Mater. Interfaces 8 (2016) 703–715.
[34] Z. Wu, Y. Xu, H. Li, Synergetic stimulation of nanostructure and chemistry cues on behaviors of fibroblasts and endothelial cells, Colloids Surf., B 160 (2017) 500–509.
[35] Y. Zhu, L. Kong, F. Farhadi, W. Xia, J. Chang, Y. He, H. Li, An injectable continuous stratified structurally and functionally biomimetic construct for enhancing osteochondral regeneration, Biomaterials 192 (2019) 149–158.
[36] W. Liu, S. Thomopoulos, Y. Xia, Electrospun nanofibers for regenerative medicine, Adv. Healthc. Mater. 1 (2012) 10–25.
[37] K. Lin, L. Xia, H. Li, X. Jiang, H. Pan, Y. Xu, W.W. Lu, Z. Zhang, J. Chang, Enhanced osteoporotic bone regeneration by strontium-substituted calcium silicate bioactive ceramics, Biomaterials 34 (2013) 10028–10042.
[38] N.S. Güldal Hoppe, A.R. Boccaccini, A review of the biological response to ionic dissolution products from bioactive glasses and glass-ceramics, Biomaterials 32 (2011) 2757–2774.
[39] M.N. Rahaman, D.E. Day, B.S. Bal, Q. Fu, S.B. Jung, L.F. Bonewald, A.P. Tomsia, Bioactive glass in tissue engineering, Acta Biomater. 7 (2011) 2355–2373.
[40] L.L. Hench, The story of Bioglass, J. Mater. Sci. Mater. Med. 17 (2006) 967–978.
[41] E. Fiume, J. Barberi, E. Verne, F. Baino, Bioactive glasses: from parent 45S5 composition to scaffold-assisted tissue-healing therapies, J. Funct. Biomater. 9 (2018) 24.
[42] X. Dong, J. Chang, H. Li, Bioglass promotes wound healing through modulating the paracrine effects between macrophages and repairing cells, J. Mater. Chem. B 5 (2017) 5240–5250.

[43] Y. Xu, J. Peng, X. Dong, Y. Xu, H. Li, J. Chang, Combined chemical and structural signals of biomaterials synergistically activate cell-cell communications for improving tissue regeneration, Acta Biomater. 55 (2017) 249–261.
[44] H. Li, K. Xue, N. Kong, K. Liu, J. Chang, Silicate bioceramics enhanced vascularization and osteogenesis through stimulating interactions between endothelia cells and bone, Biomaterials 35 (2014) 3803–3818.
[45] X. Zhuang, X. Xiang, W. Grizzle, D. Sun, S. Zhang, R.C. Axtell, S. Ju, J. Mu, L. Zhang, L. Steinman, D. Miller, H.G. Zhang, Treatment of brain inflammatory diseases by delivering exosome encapsulated anti-inflammatory drugs from the nasal region to the brain, Am. Soc. Gene Cell Ther. 19 (2011) 1769–1779.
[46] V. Luga, L. Zhang, A.M. Viloria-Petit, A.A. Ogunjimi, M.R. Inanlou, E. Chiu, M. Buchanan, A.N. Hosein, M. Basik, J.L. Wrana, Exosomes mediate stromal mobilization of autocrine Wnt-PCP signaling in breast cancer cell migration, Cell 151 (2012) 1542–1556.
[47] D. Sun, X. Zhuang, X. Xiang, Y. Liu, S. Zhang, C. Liu, S. Barnes, W. Grizzle, D. Miller, H.G. Zhang, A novel nanoparticle drug delivery system: the anti-inflammatory activity of curcumin is enhanced when encapsulated in exosomes, Am. Soc. Gene Cell Ther. 18 (2010) 1606–1614.
[48] J. Rezaie, S. Ajezi, Ç.B. Avci, M. Karimipour, M.H. Geranmayeh, A. Nourazarian, E. Sokullu, A. Rezabakhsh, R. Rahbarghazi, Exosomes and their application in biomedical field: difficulties and advantages, Mol. Neurobiol. 55 (2018) 3372–3393.
[49] M.T. Aatonen, T. Öhman, T.A. Nyman, S. Laitinen, M. Grönholm, P.R.M. Siljander, Isolation and characterization of platelet-derived extracellular vesicles, J. Extracell. Vesicles 3 (2014) 24692.
[50] Z. Luo, F. Wu, E. Xue, L. Huang, P. Yan, X. Pan, Y. Zhou, Hypoxia preconditioning promotes bone marrow mesenchymal stem cells survival by inducing HIF-1a in injured neuronal cells derived exosomes culture system, Cell Death Dis. 10 (2019) 134.
[51] M. Dao Rosova, B. Capoccia, D. Link, J.A. Nolta, Hypoxic preconditioning results in increased motility and improved therapeutic potential of human mesenchymal stem cells, Stem Cell. 26 (2008) 2173–2182.
[52] Parolini, C. Federici, C. Raggi, L. Lugini, S. Palleschi, A. De Milito, C. Coscia, E. Iessi, M. Logozzi, A. Molinari, M. Colone, M. Tatti, M. Sargiacomo, S. Fais, Microenvironmental pH is a key factor for exosome traffic in tumor cells, J. Biol. Chem. 284 (2009) 34211–34222.
[53] J.J. Ban, M. Lee, W. Im, M. Kim, Low pH increases the yield of exosome isolation, Biochem. Biophys. Res. Commun. 461 (2015) 76–79.
[54] K. Essandoh, L. Yang, X. Wang, W. Huang, D. Qin, J. Hao, Y. Wang, B. Zingarelli, T. Peng, G.C. Fan, Blockade of exosome generation with GW4869 dampens the sepsis-induced inflammation and cardiac dysfunction, Biochim. Biophys. Acta 1852 (2015) 2362–2371.
[55] B.B. Guo, S.A. Bellingham, A.F. Hill, The neutral sphingomyelinase pathway regulates packaging of the prion protein into exosomes, J. Biol. Chem. 290 (2015) 3455–3467.
[56] P. Brennwald, Reversal of fortune: do Rab GTPases act on the target membrane, J. Cell Biol. 149 (2000) 1–4.
[57] T. Tsuboi, M. Fukuda, Rab3A and Rab27A cooperatively regulate the docking step of dense-core vesicle exocytosis in PC12 cells, J. Cell Sci. 119 (2006) 2196–2203.
[58] M. Czystowska-Kuzmicz, A. Sosnowska, D. Nowis, K. Ramji, M. Szajnik, J. Chlebowska-Tuz, E. Wolinska, P. Gaj, M. Grazul, Z. Pilch, A. Zerrouqi, A. Graczyk-Jarzynka, K. Soroczynska, S. Cierniak, R. Koktysz, E. Elishaev, S. Gruca, A. Stefanowicz, R. Blaszczyk, B. Borek, A. Gzik, T. Whiteside, J. Golab, Small extracellular vesicles containing arginase-1 suppress T-cell responses and promote tumor growth in ovarian carcinoma, Nat. Commun. 10 (2019) 3000.
[59] Y. Xiao, L. Zheng, X. Zou, J. Wang, J. Zhong, T. Zhong, Extracellular vesicles in type 2 diabetes mellitus: key roles in pathogenesis, complications, and therapy, J. Extracell. Vesicles 8 (2019) 1625677.
[60] L. Zuo, Y. Xie, J. Tang, S. Xin, L. Liu, S. Zhang, Q. Yan, F. Zhu, J. Lu, Targeting exosomal EBV-LMP1 transfer and miR-203 expression via the NF-kappaB pathway: the therapeutic role of aspirin in NPC, Mol. Ther. 17 (2019) 175–184.
[61] P. Sansone, C. Savini, I. Kurelac, Q. Chang, L.B. Amato, A. Strillacci, A. Stepanova, L. Iommarini, C. Mastroleo, L. Daly, A. Galkin, B.K. Thakur, N. Soplop, K. Uryu, A. Hoshino, L. Norton, M. Bonafé, M. Cricca, G. Gasparre, D. Lyden, J. Bromberg, Packaging and transfer of mitochondrial DNA *via* exosomes regulate escape from dormancy in hormonal therapy-resistant breast cancer, Proc. Natl. Acad. Sci. U.S.A. 114 (2017) E9066–E9075.
[62] S. Lin, R.I. Gregory, MicroRNA biogenesis pathways in cancer, Nat. Rev. Canc. 15 (2015) 321–333.
[63] B. Xu, Y. Zhang, X. Du, J. Li, H. Zi, J. Bu, Y. Yan, H. Han, J.L. Du, Neurons secrete miR-132-containing exosomes to regulate brain vascular integrity, Cell Res. 27 (2017) 882–897.
[64] X. Yan, J. Cao, L. Liang, L. Wang, F. Gao, Z. Yang, J. Duan, T. Chang, S. Deng, Y. Liu, G. Dou, J. Zhang, Q. Zheng, P. Zhang, H. Han, miR-342-5p is a notch downstream molecule and regulates multiple angiogenic pathways including notch, vascular endothelial growth factor and transforming growth factor beta signaling, J. Am. Heart Assoc. 5 (2016) e003042.
[65] W.C. Zhang, T.M. Chin, H. Yang, M.E. Nga, D.P. Lunny, E.K.H. Lim, L.L. Sun, Y.H. Pang, Y.N. Leow, S.R.Y. Malusay, P.X.H. Lim, J.Z. Lee, B.J.W. Tan, N. Shyh-Chang, E.H. Lim, W.T. Lim, D.S.W. Tan, E.H. Tan, B.C. Tai, R.A. Soo, W.L. Tam, B. Lim, Tumour-initiating cell-specific miR-1246 and miR-1290 expression converge to promote non-small cell lung cancer progression, Nat. Commun. 7 (2016) 11702.
[66] J. Jin, Y. Liu, J. Si, R. Ni, J. Wang, Overexpression of miR-1290 contributes to cell proliferation and invasion of non small cell lung cancer by targeting interferon regulatory factor 2, Int. J. Biochem. Cell Biol. 95 (2018) 113–120.
[67] N. Ferrara, H.P. Gerber, J. LeCouter, The biology of VEGF and its receptors, Nat. Med. 9 (2003) 669–676.
[68] C.K. Domigan, S. Ziyad, M.L. Iruela-Arispe, Canonical and noncanonical vascular endothelial growth factor pathways: New developments in biology and signal transduction, Arterioscler. Thromb. Vasc. Biol. 35 (2015) 30–39.
[69] S. Banerjee, S.K. Dhara, M. Bacanamwo, Endoglin is a novel endothelial cell specification gene, Stem Cell Res. 8 (2012) 85–96.
[70] J.M. Barnett, S. Suarez, G.W. McCollum, J.S. Penn, Endoglin promotes angiogenesis in cell- and animal-based models of retinal neovascularization, Invest. Ophthalmol. Vis. Sci. 55 (2014) 6490–6498.
[71] K. Wu, M. Hu, Z. Chen, F. Xiang, G. Chen, W. Yan, Q. Peng, X. Chen, Asiatic acid enhances survival of human AC16 cardiomyocytes under hypoxia by upregulating miR-1290, IUBMB Life 69 (2017) 660–667.
[72] H. Li, R. Daculsi, M. Grellier, R. Bareille, C. Bourget, J. Amedee, Role of neural-cadherin in early osteoblastic differentiation of human bone marrow stromal cells cocultured with human umbilical vein endothelial cells, Am. J. Physiol. Cell Physiol. 299 (2010) C422–C430.
[73] Y. Xu, Z. Wu, X. Dong, H. Li, Combined biomaterial signals stimulate communications between bone marrow stromal cell and endothelial cell, RSC Adv. 7 (2017) 5306–5314.
[74] M. Vidal Savina, M.I. Colombo, The exosome pathway in K562 cells is regulated by Rab 11, J. Cell Sci. 115 (2002) 2505–2515.
[75] S. Guo, S. Tao, W. Yin, X. Qi, T. Yuan, C. Zhang, Exosomes derived from platelet-rich plasma promote the re-epithelization of chronic cutaneous wounds via activation of YAP in a diabetic rat model, Theranostics 7 (2017) 81–96.
[76] M. Alexander, R. Hu, M.C. Runtsch, D.A. Kagele, T.L. Mosbruger, T. Tolmachova, M.C. Seabra, J.L. Round, D.M. Ward, R.M. O'Connell, Exosome-delivered microRNAs modulate the inflammatory response to endotoxin, Nat. Commun. 6 (2015) 1–16.
[77] S. Zhu, L. Ma, S. Wang, C. Chen, W. Zhang, L. Yang, W. Hang, J.P. Nolan, L. Wu, X. Yan, Light-scattering detection below the level of single fluorescent molecules for high-resolution characterization of functional nanoparticles, ACS Nano 8 (2014) 10998–11006.
[78] H. Liu, Z. Liang, F. Wang, C. Zhou, X. Zheng, T. Hu, X. He, X. Wu, P. Lan, Exosomes from mesenchymal stromal cells reduce murine colonic inflammation via a macrophage-dependent mechanism, JCI Insight 4 (2019) e131273.
[79] L.B. Vong, T.Q. Bui, T. Tomita, H. Sakamoto, Y. Hiramatsu, Y. Nagasaki, Novel angiogenesis therapeutics by redox injectable hydrogel - regulation of local nitric oxide generation for effective cardiovascular therapy, Biomaterials 167 (2018) 143–152.